The Journal of Antibiotics (2024) 77:499–505
https://doi.org/10.1038/s41429-024-00740-4

Japan Antibiotics Research Association
The Society for Actinomycetes Japan

ARTICLE

Isolation, structural determination, and antiviral activities of a novel alanine-conjugated polyketide from *Talaromyces sp.*

Nozomi Mosu[1] · Mitsuki Yasukochi[1] · Shogo Nakajima[2,3,4] · Kou Nakamura[1] · Masaya Ogata[1] · Keita Iguchi[1] · Kazuki Kanno[1] · Tomohiro Ishikawa[5] · Kazutoshi Sugita[1] · Hironobu Murakami[1,6] · Kouji Kuramochi[7] · Tatsuo Saito[8] · Shiro Takeda[1,6] · Koichi Watashi[2,3,7] · Kan Fujino[1,6] · Shinji Kamisuki[1,6]

Received: 28 November 2023 / Revised: 26 April 2024 / Accepted: 2 May 2024 / Published online: 30 May 2024

Abstract

Antiviral agents are highly sought after. In this study, a novel alkylated decalin-type polyketide, alaspelunin, was isolated from the culture broth of the fungus *Talaromyces speluncarum* FMR 16671, and its structure was determined using spectroscopic analyses (1D/2D NMR and MS). The compound was condensed with alanine, and its absolute configuration was determined using Marfey's method. Furthermore, the antiviral activity of alaspelunin against various viruses was evaluated, and it was found to be effective against both severe acute respiratory syndrome coronavirus 2 and pseudorabies (Aujeszky's disease) virus, a pathogen affecting pigs. Our results suggest that this compound is a potential broad-spectrum antiviral agent.

Introduction

Severe acute respiratory syndrome coronavirus 2 (SARS-CoV-2) infection has resulted in enormous damage worldwide, and the total number of deaths due to coronavirus disease 2019 (COVID-19) has reached 6.9 million as of October 2023 [1]. Such emerging and reemerging viral diseases have occurred frequently in the past via transmission of viruses from animals to humans, and it is highly likely that additional infectious disease outbreaks will occur in the future. To combat emerging and reemerging viral infections, broad-spectrum antivirals (BSAs) that target multiple viruses are effective as first-line therapeutics to improve pandemic preparedness [2–4].

To date, we have explored natural products with antiviral activity from fungal metabolites and discovered various antivirals showing activity against hepatitis C virus, hepatitis B virus, and SARS-CoV-2 [5–9]. In addition to antivirals against human viruses, we have screened antivirals against animal and zoonotic viruses such as bovine leukemia virus (BLV), pseudorabies (Aujeszky's disease) virus (PRV), rabies virus, and Borna disease virus 1 [10]. In the screening programs, we demonstrated that violaceoid E and mitorubrinic acid possess antiviral activity against BLV, a retrovirus that causes enzootic bovine leukosis [11, 12]. Among the fungus-derived antivirals obtained, cell-based assays showed that neoechinulin B and vanitaracin A are

These authors contributed equally: Nozomi Mosu, Mitsuki Yasukochi

Supplementary information The online version contains supplementary material available at https://doi.org/10.1038/s41429-024-00740-4

✉ Shinji Kamisuki
kamisuki@azabu-u.ac.jp

1 School of Veterinary Medicine, Azabu University, 1-17-71 Fuchinobe, Chuo-ku, Sagamihara, Kanagawa 252-5201, Japan

2 Department of Virology II, National Institute of Infectious Diseases, 1-23-1 Toyama, Shinjuku-ku, Tokyo 162-8640, Japan

3 Research Center for Drug and Vaccine Development, National Institute of Infectious Diseases, 1-23-1, Toyama, Shinjuku-ku, Tokyo 162-8640, Japan

4 Choju Medical Institute, Yamanaka 19-14, Noyoricho, Toyohashi-shi, Aichi 441-8124, Japan

5 Graduate School of Life Science, Tokyo University of Agriculture, Sakuragaoka 1-1-1, Setagaya-ku, Tokyo 156-8502, Japan

6 Center for Human and Animal Symbiosis Science, Azabu University, 1-17-71 Fuchinobe, Chuo-ku, Sagamihara, Kanagawa 252-5201, Japan

7 Department of Applied Biological Science, Tokyo University of Science, 2641 Yamazaki, Noda, Chiba 278-8510, Japan

8 Department of Chemistry for Life Sciences and Agriculture, Faculty of Life Sciences, Tokyo University of Agriculture, Sakuragaoka 1-1-1, Setagaya-ku, Tokyo 156-8502, Japan

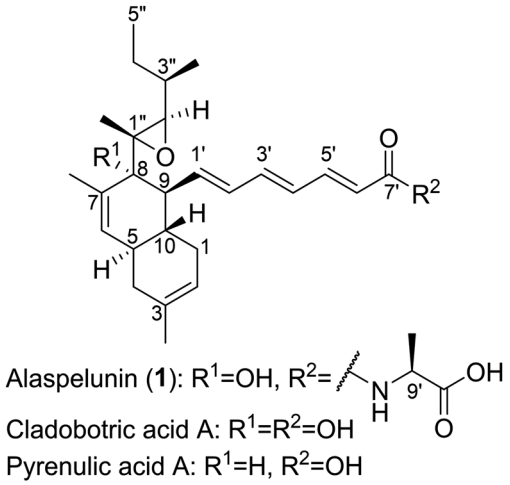

Fig. 1 Structures of alaspelunin (**1**), cladobotric acid A, and pyrenulic acid A

effective against multiple classes of viruses [6, 9, 10]. Since fungus-derived drugs such as cyclosporine A and lovastatin also exhibit antiviral activities against a wide range of viruses at least in preclinical studies, fungal metabolites may represent a good source of BSAs [3, 13]. However, few fungal metabolites have been evaluated for antiviral activity.

In the present study, we isolated the fungus *Talaromyces speluncarum* FMR 16671 from weak acid-treated sands collected at Fuchu, Tokyo, Japan. NMR and MS analyses revealed that fungal metabolite **1** was a novel alkylated decalin-type polyketide that was condensed with alanine (Fig. 1). In addition, compound **1** exhibited anti-SARS-CoV-2 and anti-PRV activities. PRV, an alpha herpesvirus, causes neurological and respiratory diseases in pigs, which results in economic losses in the swine industry worldwide [14]. Although PRV causes fatal neurological symptoms in non-pig hosts, its pathogenicity in humans remains unclear. However, a novel PRV variant strain was recently isolated from cerebrospinal fluid in a human case of acute encephalitis in China, which implies the great risk of PRV transmission from pigs to humans; thus, antiviral drugs are required to control PRV infection [15]. Herein, we describe the structural elucidation along with the anti-SARS-CoV-2 and anti-PRV activities of **1**.

Results and discussion

The culture broth of *T. speluncarum* FMR 16671 was extracted using CH_2Cl_2, and the crude extract was subjected to TLC-guided fractionation to obtain compound **1**. The molecular formula of compound **1** was determined to be $C_{29}H_{41}NO_5$ using HRMS (FAB). The IR spectrum indicated the presence of hydroxy (3328 cm^{-1}) and carbonyl (1727 and 1649 cm^{-1}) groups. The ^{13}C NMR and DEPT spectra suggested the presence of six quaternary carbons, 14 methine carbons, three methylene carbons, and six methyl carbons (Table 1 and Fig. S2 and S3). The consecutive ^1H-^1H COSY correlations from H-1′ to H-6′ established a triene side-chain moiety (Fig. 2a and S4), and the configuration was determined to be all-*trans* based on the coupling constants (14.6–14.9 Hz, Table 1 and Fig. S1). The ^1H-^1H COSY correlation between N-H and H-9′, and the HMBC correlations from Me-9′ to C-9′ and C-10′ (δ 175.4) suggested the presence of an alanine moiety (Fig. 2a and S6). The alanine moiety was found to connect to the triene side

Table 1 ^1H NMR (400 MHz, $CDCl_3$) and ^{13}C NMR (100 MHz, $CDCl_3$) data for compound 1

	1			
Pos.	δ_C	Type	δ_H	mult (*J* in Hz)
1	31.8	CH_2	1.95	m
			1.49	m
2	121.2	CH	5.36	brs
3	133.9	C		
3-Me	23.3	CH_3	1.66	s
4	37.1	CH_2	2.06	m
			1.79	m
5	38.4	CH	2.06	m
6	132.7	CH	5.58	brs
7	133.5	C		
7-Me	18.1	CH_3	1.72	s
8	75.6	C		
9	58.9	CH	2.34	dd (10.9, 11.6)
10	38.0	CH	1.92	m
1'	136.7	CH	5.95	dd (10.9, 14.6)
2'	133.2	CH	6.15	dd (10.8, 14.6)
3'	140.0	CH	6.60	dd (10.8, 14.8)
4'	128.8	CH	6.19	dd (11.3, 14.8)
5'	142.2	CH	7.23	dd (11.3, 14.9)
6'	122.2	CH	5.90	d (14.9)
7'	166.7	C		
8'		NH	6.65	d (7.0)
9'	48.4	CH	4.64	m
9'-Me	18.0	CH_3	1.47	d (7.1)
10'	175.4	C		
1"	63.0	C		
1"-Me	15.4	CH_3	1.39	s
2"	63.2	CH	3.02	d (8.5)
3"	34.3	CH	1.31	m
3"-Me	15.3	CH_3	0.94	m
4"	27.8	CH_2	1.62	m
			1.32	m
5"	11.1	CH_3	0.94	m

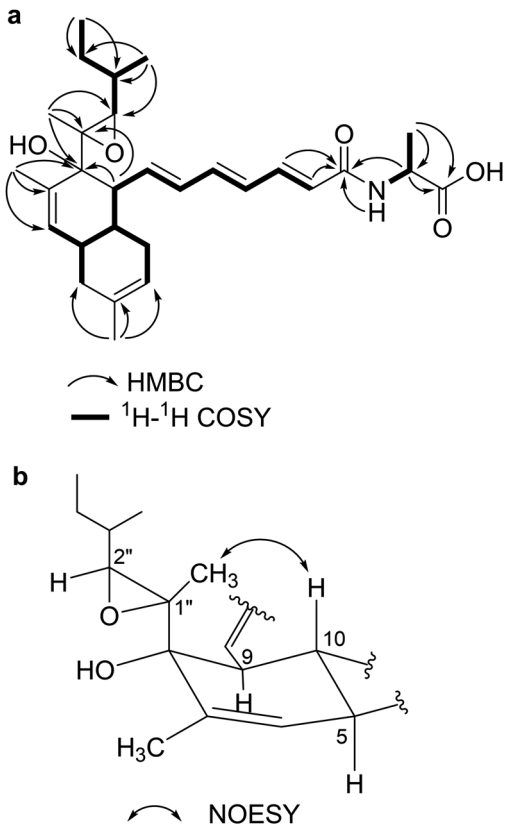

Fig. 2 **a** Key ^{1}H–^{1}H COSY and HMBC correlations for **1**. **b** Key NOESY correlation for **1**

chain via an amide bond, based on HMBC correlations from H-5′, H-6′, N-H, and H-9′ to C-7′. The HMBC correlations from Me-7 to olefinic carbon C-6 and C-7 and from Me-3 to olefinic carbon C-2 and C-3 along with ^{1}H-^{1}H COSY correlations revealed the tetradehydrodecalin system. The epoxide-containing side chain was established based on the consecutive ^{1}H-^{1}H COSY correlations from H-2″ to H-5″ and HMBC correlations from Me-1″ to C-8, C-1″, and C-2″. The proposed structure of **1** is a novel alanine-conjugated derivative of cladobotric acid A, which was previously isolated from the fungus *Cladobotryum* sp., and **1** was named alaspelunin (Fig. 1). All proton and carbon signals of **1** were assigned using ^{1}H-^{1}H COSY, HMQC and HMBC analyses (Table 1 and Fig. 2 and S4–S6) [16].

The ^{1}H and ^{13}C NMR data for **1** were in good agreement with those of cladobotric acid A, except for the alanine moiety, which suggested that the relative configuration of **1** was also similar to that of cladobotric acid A [16]. The NOESY spectrum and values of the coupling constants supported the relative configurations (Table 1 and Fig. 2b and S7). The typical trans-diaxial coupling constant ($J_{\text{H-9/H-10}} = 11.6$ Hz) and absence of NOESY correlations between H-9 and H-10 indicated an anti-relationship between C-9 and C-10. A NOESY correlation was observed between Me-1″ and H-10, whereas no NOESY correlations were observed between H-5 and H-10 and between Me-1″ and H-2″, which suggested that the relative configurations of tetradehydrodecalin and epoxide-containing side chain of **1** were identical to those of cladobotric acid A. In addition, the ^{1}H and ^{13}C NMR and NOESY data of **1** were in agreement with those of pyrenulic acid A, a compound closely related to cladobotric acid A (Fig. 1) [17]. Compound **1**, cladobotric acid A, and pyrenulic acid A showed a negative specific rotation [compound **1**: $[\alpha]^{26}_{D}$ –47 (*c* 0.26, $CHCl_3$); cladobotric acid A: $[\alpha]^{26}_{D}$ –87 (*c* 0.11, $CHCl_3$); pyrenulic acid A: $[\alpha]^{26}_{D}$ –82 (*c* 0.85, $CHCl_3$)], and specific rotations of all cladobotric acid A-related compounds, including cladobotric acids B–I, are also negative [16–18]. These data suggested that the absolute configuration of the polyketide moiety in **1** is identical to that of these compounds. The absolute configuration of the alanine moiety of **1** was determined using Marfey's method. The hydrolysates of **1**, as well as L-Ala and D-Ala, were derivatized using L-FDLA, and the obtained Marfey derivatives were analyzed via LC-MS. Since Marfey's derivative of hydrolysate **1** showed the same retention time as L-Ala, the alanine moiety of **1** was determined to be L-Ala (Fig. S8). Furthermore, we calculated electronic circular dichroism (ECD) spectra of possible stereoisomers (5*R*,8*R*,9*S*,10*R*,9′*S*,1″*S*,2″*R*,3″*R*)-**1** and (5*S*,8*S*,9*R*,10*S*,9′*S*,1″*R*,2″*S*,3″*S*)-**1a** using TD-DFT at the cam-B3LYP/6-311 + + G(2d,p) level (Fig. S9). The calculated ECD spectrum of **1** matched the experimental data well. Hence, we conclude that alaspelunin has the 5*R*,8*R*,9*S*,10*R*,9′*S*,1″*S*,2″*R*,3″*R* absolute configuration.

To elucidate the bioactivity of **1**, its antiviral activity against SARS-CoV-2, PRV, BLV, and herpes simplex virus-1 was evaluated. The results showed that compound **1** exhibited anti-SARS-CoV-2 and anti-PRV activities. Compound **1** reduced the viral RNA of SARS-CoV-2 in a dose-dependent manner, and the IC_{50} and IC_{90} values were 11.9 and 40.0 μM, respectively (Fig. 3a and S10). We also confirmed that **1** induced no cytotoxicity in Vero E6/TMPRSS2 cells at concentrations of up to 100 μM (Fig. 3b).

The anti-PRV activity of compound **1** was assessed via plaque assays using porcine kidney-derived PK-15 cells. Treatment with 10 and 25 μM **1** significantly reduced PRV plaque size (Fig. 4a and S11). Compound **1** did not show cytotoxicity in PK-15 cells at concentrations up to 50 μM (Fig. 4b).

In this study, we revealed that alaspelunin (**1**) is a novel L-alanine-conjugated decalin-type polyketide. Most cladobotric acid derivatives possess a side chain of triene carboxylic acid, whereas only cladobotric acid F is a methyl ester [16, 18]. The side chains of other related compounds, including pyrenulic acids A and B, F2928-1, and hakuhybotric acid, also comprise triene carboxylic acid; however, no amino acid-conjugated derivatives have been reported

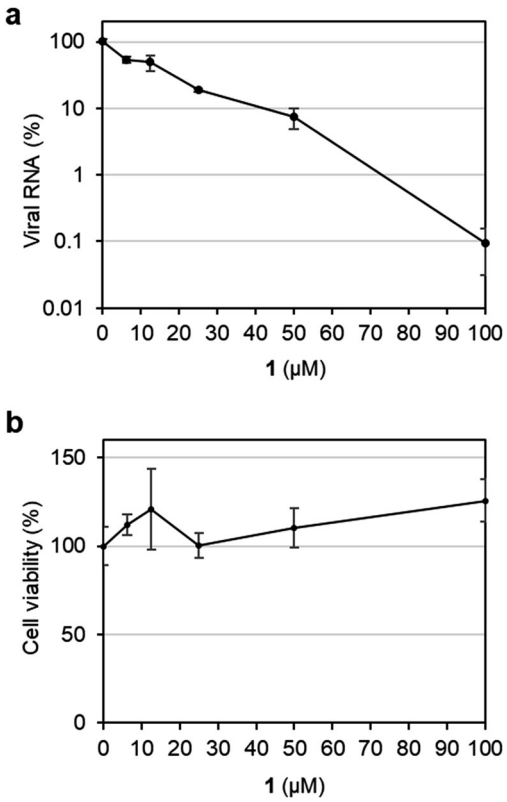

Fig. 3 Anti-SARS-CoV-2 activity of **1**. **a** Extracellular SARS-CoV-2 RNA in Vero E6/TMPRSS2 cells was quantified after treatment with the compound (6.25, 12.5, 25, 50, and 100 μM) during 1 h of virus inoculation and 24 h after inoculation. **b** The viability of Vero E6/TMPRSS2 cells was measured using the cytotoxicity assay described in the EXPERIMENTAL SECTION. SARS-CoV-2, severe acute respiratory syndrome coronavirus 2

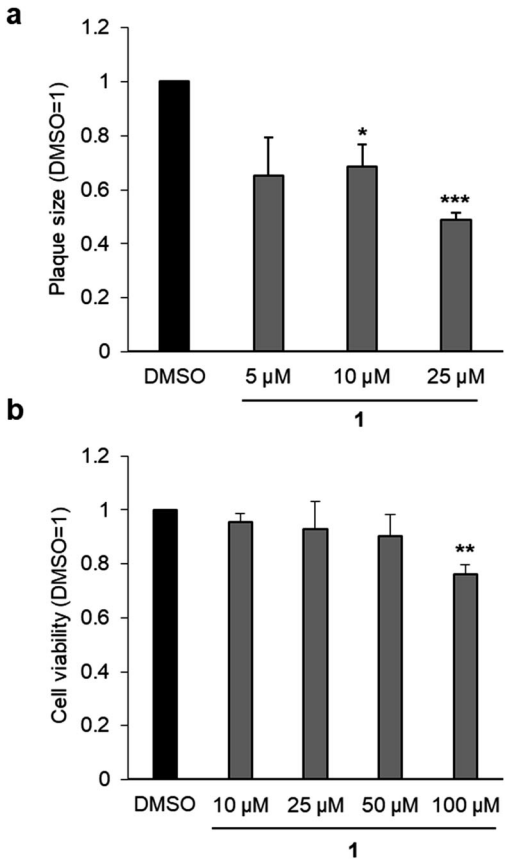

Fig. 4 Anti-PRV activity of **1**. **a** PK-15 cells were treated with **1** (5, 10, or 25 μM) for 24 h, and the supernatant was removed. The cells were inoculated with PRV for 1 h and then cultured in agar maintenance medium containing **1** (5, 10, or 25 μM) for 2 d. After incubation, the cells were fixed and plaque size was measured. **b** PK-15 cell viability was measured via cytotoxicity assays as described in the EXPERIMENTAL SECTION. Values are presented as the mean ± standard deviation from three independent experiments. Statistical significance was analyzed using a two-tailed *t*-test. $^{*}P < 0.05$, $^{**}P < 0.01$, $^{***}P < 0.001$ compared with DMSO control (0 μM). PRV, pseudorabies virus

[17, 19, 20]. To the best of our knowledge, there are no reports of polyketides containing triene carboxylic acids that form amide bonds with alanine.

Herein, we revealed that **1** exhibited both anti-SARS-CoV-2 and anti-PRV activities. Cladobotric acids possess antibacterial activity and other related compounds, including hakuhybotric acid and its derivative hakuhybotrol, show antifungal activity, while pyrenulic acids show DNA polymerase inhibitory activity; however, no studies have investigated the antiviral activity of these related compounds [17–19, 21].

Pigs serve as the natural host for PRV; however, PRV has been reported to cause human endophthalmitis and encephalitis. A human-derived PRV strain was isolated from an acute human encephalitis case in 2020 [15, 22, 23]. These cases suggest the possibility of pig-to-human transmission of PRV and a potential threat to human public health. Treatment of PRV-induced human encephalitis with the anti-herpes virus drug acyclovir shows limited efficacy; thus, novel anti-PRV drugs are needed. Since the isolation of PRV from a human case, anti-PRV small molecules have been sought after, and several anti-PRV compounds, including natural compounds, have been discovered recently [24–30]. Alaspelunin (**1**) is a novel anti-PRV natural product that has the potential to serve as a lead compound for the development of anti-PRV drugs. Furthermore, compound **1** exhibited both anti-SARS-CoV-2 and anti-PRV activities, suggesting that this compound may represent a candidate for the development of BSAs. Future studies should examine the antiviral spectrum and mechanism of action of **1**.

Materials and methods

General experimental procedures

Optical rotations were recorded using a JASCO P-2200 digital polarimeter at room temperature. UV spectra were

obtained using a UVmini-1240 spectrophotometer (Shimadzu). The IR spectra were recorded using a JASCO FT/IR-4600 spectrophotometer and reported as wavenumbers (cm^{-1}). ^{1}H and ^{13}C NMR spectra were recorded using a Bruker 400 MHz spectrometer (Avance DRX-400) using $CDCl_3$ solution (with tetramethylsilane (TMS) for ^{1}H NMR and $CDCl_3$ for ^{13}C NMR as an internal reference). Chemical shifts were expressed in δ (ppm) relative to TMS or residual solvent resonance, and coupling constants (J) were expressed in Hz. HRFAB-MS analysis was performed using a JEOL mass spectrometer (JMS-700). LC-MS experiments were performed using a GL Science LC800 system coupled with an AB Sciex API3200 QTRAP spectrometer. ECD spectra were recorded in MeOH at a concentration of 2.0×10^{-4} M and at 23 °C using a JASCO J-725 CD spectrometer with 2-mm path-length cuvettes.

Isolation and cultivation of fungi

Sand samples were collected from Fuchu, Tokyo, Japan and suspended in sterilized 5% aqueous acetic acid solution. The suspension was spread on potato dextrose agar (PDA) plates (Difco & BBL) and incubated for 1–2 weeks at 37 °C. Fungi growing on these plates were transferred to individual PDA plates and cultured under the same conditions. Cultures were repeated several times to obtain pure strains. The fungus strain that produced alaspelunin in the present study was identified as *T. speluncarum* FMR 16671 (GenBank accession number NG_075220.1) with 98% sequence similarity, based on the sequence of the 5′ end of the large subunit rRNA gene (D1/D2 region) of 26/28 S rRNA [31].

Extraction and isolation

The isolated fungal strain was cultured by transferring a small piece of agar from the culture plate to five two-liter Erlenmeyer flasks, each containing potato dextrose broth (24 g; Difco & BBL) in 1 l H_2O. The culture (5 l) was grown under static conditions at room temperature in the dark for 22 d. The culture broth was filtered through cheesecloth to remove fungal mycelia, and the filtrate was extracted using CH_2Cl_2. The organic layer was evaporated *in vacuo* to obtain a crude extract (501 mg), which was subsequently separated via silica gel column chromatography using $CHCl_3$-MeOH (99:1–90:10) to yield fractions 1–4. Fraction 4 was separated via silica gel column chromatography using hexane-EtOAc (1:2, a solution containing 0.5% acetic acid) and EtOAc (a solution containing 0.5% acetic acid) to yield compound **1** (61.4 mg). The purity of compound **1** was confirmed to be > 95% using HPLC.

Alaspelunin (1): Brown oil; $[\alpha]^{26}_{D}$ –47 (*c* 0.26, $CHCl_3$); UV λ^{MeOH}_{max} nm (ε) 301 (23,400); ECD (c 2.0×10^{-4}, MeOH) Δε (nm) +1.34 (290), −1.05 (235); IR ν_{max} (film) cm^{-1} 3328, 2961, 2928, 2872, 1727, 1649, 1456, 1005; HRMS (FAB) *m/z* 484.3065 $[M + H]^+$ (calcd for $C_{29}H_{42}NO_5$, 484.3063); ^{1}H and ^{13}C data, see Table 1.

Marfey's analysis

Compound **1** (50 μg) was hydrolyzed using 6 M HCl (200 μl) at 110 °C for 16 h in a Teflon-sealed Ace pressure tube, and the reaction mixture was evaporated to dryness by blowing nitrogen gas. The dried hydrolysate, L-Ala (0.2 mg), and D-Ala (0.2 mg) were transferred to an Ace pressure tube and dissolved in water (100 μl). Subsequently, 0.1 M $NaHCO_3$ (20 μl) and L-FDLA in acetone (1 mg in 100 μl) were added to the solution, and each tube was sealed and heated at 50 °C for 40 min. After addition of 1 M HCl (20 μl) to quench the reaction, the reaction mixture was evaporated by blowing nitrogen gas. The dried mixture was dissolved in 35% aqueous MeOH containing 0.1% formic acid, and then analyzed via LC-MS using a reversed-phase column (Shimazu shim-pack GIST C18, 2.1 × 100 mm, 5 μm) eluted with 35–90% aqueous MeOH containing 0.1% formic acid at a flow rate of 0.2 ml/min over 30 min.

Cell culture

Vero E6/TMPRSS2 cells overexpressing the transmembrane serine protease 2 gene were cultured in Dulbecco's modified Eagle's medium supplemented with 10% fetal bovine serum (FBS), 100 units ml^{-1} penicillin, 100 μg ml^{-1} streptomycin, 10 mM HEPES (pH 7.4), and 1 mg ml^{-1} G418 at 37 °C in 5% CO_2. During the infection assay, G418 was removed and 10% FBS was replaced with 2% FBS. PK15 cells were cultured in Dulbecco's modified Eagle's medium supplemented with 10% FBS and antibiotic mixture (20 IU ml^{-1} penicillin and 0.1 mg ml^{-1} streptomycin) at 37 °C in 5% CO_2. During the infection assay, 10% FBS was removed.

Anti-SARS-CoV-2 activity assay

SARS-CoV-2 was handled in a biosafety level 3 laboratory. SARS-CoV-2 Wk-521 strain (2019-hCoV/Japan/TY/WK-521/2020) was inoculated at a multiplicity of infection of 0.003 into Vero E6/TMPRSS2 cells for 1 h and washed. The supernatant of the cells cultured for another 24 h was recovered, and the presence of extracellular viral RNA was determined. Compound **1** was added during viral inoculation for 1 h and post-inoculation for 24 h. Remdesivir was used as a positive control [32].

Quantification of viral RNA

Viral RNA was extracted using a MagMAX Viral/Pathogen II Nucleic Acid Isolation Kit (Thermo Fisher Scientific) and

quantified via real-time reverse transcription polymerase chain reaction (RT-PCR) analysis using the THUNDERBIRD Probe One-step qRT-PCR kit (Toyobo). The following primers were used: 5′-ACAGGTACGTTAATAGTTAATAGCGT-3′ and 5′-ATATTGCAGCAGTACGCACACA-3′; 5′-FAM-ACACTAGCCATCCTTACTGCGCTTCG-TAMRA-3′ was used as a probe as previously described [9].

Viability of Vero E6/TMPRSS2 cells

Cell viability was determined via a cytotoxicity assay using cell-counting kit-8 (Dojindo Laboratories) as previously described [9].

Anti-PRV activity assay

PK-15 cells were seeded into six-well plates. After reaching 90% confluence, the cells were treated with various concentrations of **1** or 500 μM acyclovir and incubated in a 5% CO_2 incubator at 37 °C for 24 h. After incubation, the supernatant was removed, and the cells were inoculated with PRV at 40–70 plague-forming units/well. After viral attachment for 1 h, the PK-15 cells were washed twice with maintenance medium and subsequently cultured in agar maintenance medium containing various concentrations of **1** or 500 μM acyclovir in a 5% CO_2 incubator at 37 °C for 2 d. After incubation, cells were fixed and stained with a solution of 4% paraformaldehyde and a mixture of 22% EtOH-0.8% crystal violet. The plaque size was measured. Cell viability at 72 h post-treatment was measured using an MTT assay. Statistical significance was analyzed using a two-tailed *t*-test conducted using the built-in statistical functions of MS Excel. The cutoff for significance was set at $P < 0.05$.

Acknowledgements We acknowledge the support from Dr. Takayuki Kamihara and the Materials Analysis Division, Open Facility Center, Tokyo Institute of Technology for NMR analysis, and Mr. Makoto Roppongi and center for Instrumental Analysis, Utsunomiya University for CD analysis. The computation was performed by the Research Center for Computational Science, Okazaki, Japan (Project: 23-IMS-C090). This work was partially supported by grants-in-aid from the Japan Society for the Promotion of Science (KAKENHI 18K05343, 20H03499, and 21K05299), grants from the Japan Agency for Medical Research and Development (JP20fk0210036, JP22fk0310504, JP22ama121007, and JP22fk0108529), the Terumo Life Science Foundation, the Japan Foundation for Applied Enzymology, and the Center for Human and Animal Symbiosis Science and Center for Diversity, Equity & Inclusion, Azabu University.

Compliance with ethical standards

Conflict of interest The authors declare no competing interests.

References

1. https://covid19.who.int/ (accessed 17 Oct 2023).
2. Andersen PI, et al. Discovery and development of safe-in-man broad-spectrum antiviral agents. Int J Infect Dis. 2020;93:268–76.
3. Ianevski A, et al. Novel activities of safe-in-human broad-spectrum antiviral agents. Antiviral Res. 2018;154:174–82.
4. Adamson CS, et al. Antiviral drug discovery: preparing for the next pandemic. Chem Soc Rev. 2021;50:3647–55.
5. Matsunaga H, et al. Isolation and structure of vanitaracin A, a novel anti-hepatitis B virus compound from Talaromyces sp. Bioorg Med Chem Lett. 2015;25:4325–8.
6. Nakajima S, et al. Fungus-derived neoechinulin B as a novel antagonist of liver X receptor, identified by chemical genetics using a hepatitis C virus cell culture system. J Virol. 2016;90:9058–74.
7. Nakamura K, et al. Identification of methylsulochrin as a partial agonist for Aryl hydrocarbon receptors and its antiviral and anti-inflammatory activities. Chem Pharm Bull (Tokyo). 2023;71:650–4.
8. Nishikori S, et al. Anti-hepatitis C virus natural product from a fungus, penicillium herquei. J Nat Prod. 2016;79:442–6.
9. Nishiuchi K, et al. Synthesis and antiviral activities of neoechinulin B and Its derivatives. J Nat Prod. 2022;85:284–91.
10. Kamisuki S, et al. Isolation, structural determination, and antiviral activities of metabolites from vanitaracin A-producing talaromyces sp. J Antibiot (Tokyo). 2023;76:75–82.
11. Murakami H, et al. Specific antiviral effect of violaceoid E on bovine leukemia virus. Virology. 2021;562:1–8.
12. Murakami H, et al. Development of a novel fluorogenic assay method for screening inhibitors of bovine leukemia virus protease and identification of mitorubrinic acid as an anti-BLV compound. Biosci Biotechnol Biochem. 2023;87:946–53.
13. Ji X, Li Z. Medicinal chemistry strategies toward host targeting antiviral agents. Med Res Rev. 2020;40:1519–57.
14. Pomeranz LE, Reynolds AE, Hengartner CJ. Molecular biology of pseudorabies virus: impact on neurovirology and veterinary medicine. Microbiol Mol Biol Rev. 2005;69:462–500.
15. Liu Q, et al. A novel human acute encephalitis caused by pseudorabies virus variant strain. Clin Infect Dis. 2021;73:e3690–e3700.
16. Mitova MI, et al. Cladobotric acids A-F: new cytotoxic polyketides from a New Zealand Cladobotryum sp. J Org Chem. 2006;71:492–7.
17. Le DH, Takenaka Y, Hamada N, Mizushina Y, Tanahashi T. Polyketides from the cultured lichen mycobiont of a Vietnamese Pyrenula sp. J Nat Prod. 2014;77:1404–12.
18. Dao TT, et al. Cladobotric acids: metabolites from cultures of cladobotryum sp., semisynthetic analogues and antibacterial activity. J Nat Prod. 2022;85:572–80.
19. Watanabe Y, et al. Hakuhybotric acid, a new antifungal polyketide produced by a mycoparasitic fungus hypomyces pseudocorticiicola FKI-9008. J Gen Appl Microbiol. 2022;68:200–6.
20. Kanai Y, et al. F2928-1 and −2, New Antifungal Antibiotics From Cladobotryum sp. J Antibiot (Tokyo). 2005;58:507–13.
21. Watanabe Y, et al. Hakuhybotrol, a polyketide produced by hypomyces pseudocorticiicola, characterized with the assistance of 3D ED/MicroED. Org Biomol Chem ED/MicroED. 2023;21:2320–30.
22. Yang X, et al. Characteristics of human encephalitis caused by pseudorabies virus: a case series study. Int J Infect Dis. 2019;87:92–9.
23. Ai JW, et al. Human endophthalmitis caused by pseudorabies virus infection, China, 2017. Emerg Infect Dis. 2018;24:1087–90.

24. Hu H, et al. Myricetin inhibits pseudorabies virus infection through direct inactivation and activating host antiviral defense. Front Microbiol. 2022;13:985108.
25. Andreu S, Ripa I, Praena B, López-Guerrero JA, Bello-Morales R. The valproic acid derivative valpromide inhibits pseudorabies virus infection in swine epithelial and mouse neuroblastoma cell lines. Viruses. 2021;13:2522.
26. Wang C, et al. A bivalent beta-carboline derivative inhibits macropinocytosis-dependent entry of pseudorabies virus by targeting the kinase DYRK1A. J. Biol. Chem. 2023;299:104605.
27. Bo Z, et al. Identification of Na+/K+-ATPase inhibitor bufalin as a novel pseudorabies virus infection inhibitor in vitro and in vivo. Int J Mol Sci. 2023;24:14479.
28. Liu M, et al. Antiviral activity of benzoheterocyclic compounds from soil-derived streptomyces Jiujiangensis NBERC-24992. Molecules. 2023;28:878.
29. Zhang Y, et al. Napyradiomycin A4 and its relate compounds, a new anti-PRV agent and their antibacterial activities, from streptomyces kebangsaanensis WS-68302. Molecules. 2023;28:640.
30. Sun Y, et al. Quercetin as an antiviral agent inhibits the pseudorabies virus in vitro and in vivo. Virus Res. 2021;305:198556.
31. Wang X, et al. Identification of clinically relevant fungi and prototheca species by rRNA gene sequencing and multilocus PCR coupled with electrospray ionization mass spectrometry. PLoS One. 2014;9:e98110.
32. Yin W, et al. Structural basis for inhibition of the RNA-dependent RNA polymerase from SARS-CoV-2 by Remdesivir. Science. 2020;368:1499–504.